Persistence of Surface Domain Structures for a Bulk Ferroelectric above T_C

A. Höfer,[1,*] M. Fechner,[2,3,†] K. Duncker,[1] M. Hölzer,[2] I. Mertig,[1,2] and W. Widdra[1,2]

[1]*Institute of Physics, Martin-Luther-Universität Halle-Wittenberg, D-06099 Halle, Germany*
[2]*Max Planck Institute of Microstructure Physics, Weinberg 2, D-06120 Halle, Germany*
[3]*Department for Material Theory, ETH Zürich, CH-8093 Zürich, Switzerland*

(Received 25 July 2011; published 24 February 2012)

Photoemission electron microscopy performed on a well-prepared surface of $BaTiO_3$ reveals the persistence of surface domains at temperatures well above the bulk Curie temperature. Their patterns follow the ferroelectric domain structure observed at 300 K. The contrast between formerly outward polarized domains and in-plane polarized domains is preserved across the transition, while the contrast of inward polarized domains changes sign. The work functions of different possible structures are compared by first-principles calculations. The domain contrast in photoemission above the bulk Curie temperature is associated with a remaining tetragonal distortion of the topmost unit cells which is stabilized by an ionic surface relaxation.

DOI: 10.1103/PhysRevLett.108.087602 PACS numbers: 77.80.Dj, 68.35.B−, 68.37.Xy, 68.47.Gh

The different properties of solid surfaces and interfaces compared to the bulk have been technically applied in various semiconductor devices for decades. Very recently, many studies have addressed the interface properties of oxides, because novel phenomena are observed and furthermore expected for this class of strongly correlated materials. On the one hand, the unique interfacial electron system offers the potential for future applications as recently reviewed by Mannhart and Schlom [1]. On the other hand, the functionality of oxides, like ferroelectricity, can also be used in new ways by adequate realization of interfaces. For example, Tsymbal and Kohlstedt proposed tunnel junctions with an ultrathin ferroelectric barrier for use in memory devices [2]. Furthermore, in the emerging field of multiferroics, layered heterostructures consisting of a sequence of thin magnetic and ferroelectric films are highly promising [3,4]. For all these applications, a well-controlled interface and an understanding of the fundamental interfacial effects are required.

An important class of ferroelectric materials are the perovskites with $BaTiO_3$ (BTO) as a famous representative showing a spontaneous polarization of 26 $\mu C/cm^2$ at room temperature. In BTO, the electric polarization is due to relative displacements of the oxygen atoms with respect to the cations. Already in the very first studies on BTO, differences between the ferroelectric properties of the crystal surface and the interior were found [5]. Anomalies in switching experiments observed by Merz [6] were explained for the first time by Drougard and Landauer in terms of a dead layer [7], which was picked up and refined by several other groups. The microscopic origin of this dead layer is still under debate, which demonstrates that there exist open questions concerning the structure and the resulting ferroelectric properties of perovskite surfaces [8]. Even the surface of the paraelectric perovskite $SrTiO_3$ shows extraordinary properties. Santander-Syro *et al.* demonstrated very recently the formation of a 2D electron gas at the surface-vacuum interface [9].

In this Letter, we present the ferroelectric domain structure at the very surface of a BTO single crystal investigated by photoelectron emission microscopy (PEEM), since this technique is sensitive to the ferroelectric response solely from the topmost layers of the sample [10,11]. To address the surface-near ferroelectric properties, the preparation of a chemically clean and well-ordered surface is a prerequisite and has been realized by mild Ar^+ sputtering, annealing in 10^{-5} mbar O_2 to 1000 K, and final flashing to 1370 K in ultrahigh vacuum (UHV). The resulting low energy electron diffraction (LEED) pattern in Fig. 1(a) shows sharp and intensive (1×1) spots indicating a well and long-range ordered surface. The x-ray photoelectron spectra (not shown here) reveal the correct $BaTiO_3$ composition and exclude any contamination of the sample. As a light source for the PEEM experiments, a femtosecond laser system in combination with a noncollinear optical

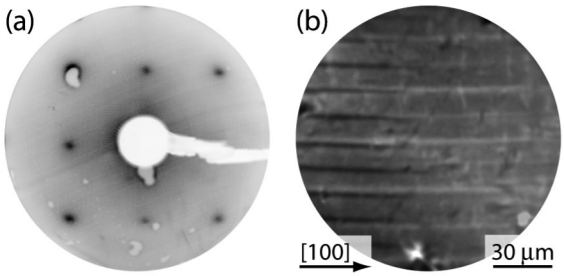

FIG. 1. (a) LEED and (b) PEEM of the BTO(001) surface after UHV preparation [(a) $E = 60$ eV, $T = 300$ K; (b) FOV = 150 μm, $h\nu = 4.35$ eV, approximately 330 K]. The sample reveals a stripelike domain pattern consisting of all three domain types, discriminable by their different photoemission yields.

parametric amplifier was used, and the output is frequency-doubled for photoexcitation of the sample surface [10].

The ferroelectric domain structure of a BTO(001)-(1×1) surface recorded by PEEM with a field of view (FOV) of 150 μm at approximately 330 K is shown in Fig. 1(b). PEEM images measured at room temperature exhibit the same stripelike domain pattern oriented along one of the $\langle 100 \rangle$ high-symmetry directions. Basically, one can discriminate two different contrast sequences: one in the left part of the image consisting of gray and dark stripes and one in the right part consisting of gray and bright stripes. The contrast differences originate directly from work function changes caused by the different alignment of the electric polarization. At the (001) surface of tetragonal BTO, there are three distinct projections of the electric polarization, which are parallel ($P_\uparrow$), antiparallel ($P_\downarrow$), or perpendicular ($P_\rightarrow$) to the surface normal. The in-plane $P_\rightarrow$ state is fourfold degenerate as the $[\pm 100]$ and $[0 \pm 10]$ directions are equivalent. The outward (inward) directed dipole moment of $P_\uparrow$ ($P_\downarrow$) domains results in a lowered (increased) work function as compared to the $P_\rightarrow$ domains [12]. Therefore, the domain pattern on the left in Fig. 1(b) is a sequence of $P_\downarrow$-$P_\rightarrow$ domains and on the right is a sequence of $P_\uparrow$-$P_\rightarrow$ domains. For this assignment it is important that external screening charges by adsorbates [12] can be ruled out due to the sample preparation. Furthermore, we can exclude internal screening, since no band bending is detectable in photoemission spectroscopy.

In Figs. 2(a)–2(d), the temperature dependence of the surface domain structure is shown. The domain configuration at room temperature as depicted in Fig. 2(a) reveals a sequence of broad $P_\rightarrow$ and narrow $P_\downarrow$ domains which depends on the local strain within the sample. Upon heating, this pattern stays constant, as exemplarily shown in Fig. 2(b), until a temperature of 398 K is reached. There, an abrupt transition to a new domain configuration takes place. Compared to the stable pattern between room temperature and about 395 K [Figs. 2(a) and 2(b)], the new pattern [Fig. 2(c)] exhibits an inverted contrast but is otherwise similar. Upon further heating of the sample, the pattern remains fixed but with continuously decreasing contrast until a temperature of approximately 510 K is reached, where no pattern is any longer observable as can be seen in Fig. 2(d).

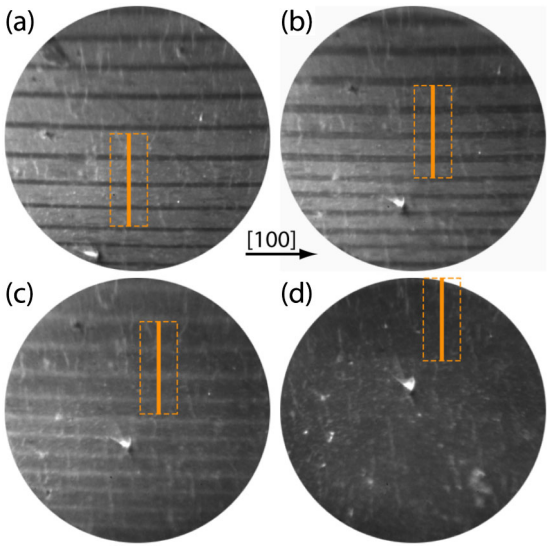

FIG. 2 (color online). (a)–(d) PEEM images of a $P_\downarrow$-$P_\rightarrow$ domain sequence measured at different temperatures: (a) 305, (b) 373, (c) 399, and (d) 513 K (FOV = 150 μm, $h\nu = 4.35$ eV). The dashed rectangle indicates the position where a line profile perpendicular to the domain pattern is taken.

The evolution of the domain structure between 304 and 523 K is illustrated in Fig. 3(a). It shows a vertical line scan of the PEEM images in Figs. 2(a)–2(d) as a function of the sample temperature. From room temperature up to approximately 370 K, no significant change of the domain pattern is observed. However, a further increase in temperature leads to a lateral movement of the domain walls accompanied by a broadening of the $P_\downarrow$ domains. At T_C, a contrast inversion takes place, and this new domain pattern is preserved up to 510 K with decreasing contrast.

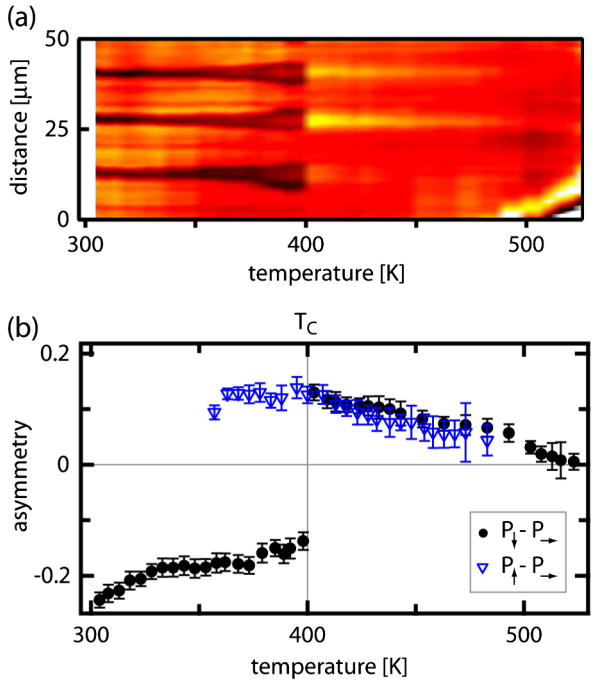

FIG. 3 (color online). (a) Line profiles of PEEM images along the yellow bar indicated in Figs. 2(a)–2(d) are strung together to illustrate the evolution of the domain structure over a wide temperature range. The profiles are normalized to the photoemission signal from the $P_\rightarrow$ domains. (b) Temperature dependence of the asymmetry between $P_\downarrow$ and $P_\rightarrow$ domains (black dots) and $P_\uparrow$ and $P_\rightarrow$ domains (open blue triangles). The $P_\uparrow$-$P_\rightarrow$ data set has been measured with $h\nu = 4.27$ eV and is scaled by a factor of 1.5 for better comparison. Please note that, in general, the observed asymmetry depends on the photon energy as well as on the surface preparation itself.

Quantitatively, this is depicted in Fig. 3(b) by black dots where the asymmetry A in the photoemission yield N of (former) $P_{\downarrow}$ and $P_{\rightarrow}$ domains is shown as

$$A = \frac{N_{\downarrow} - N_{\rightarrow}}{N_{\downarrow} + N_{\rightarrow}}.$$

A similar experiment starting from a $P_{\uparrow}$-$P_{\rightarrow}$ domain configuration is represented by the open blue triangles in Fig. 3(b). The asymmetry remains approximately constant up to T_C and also continuously decreases at higher temperatures but without inversion at T_C. Irrespective of the absolute values, the trend is the same as for the $P_{\downarrow}$-$P_{\rightarrow}$ domain configuration. In all experiments we find that, independent of whether the domain pattern at room temperature consists of a $P_{\downarrow}$-$P_{\rightarrow}$ or a $P_{\uparrow}$-$P_{\rightarrow}$ sequence, at temperatures above the Curie point the formerly darker $P_{\downarrow}$ and brighter $P_{\uparrow}$ domains show always a higher photoemission intensity than the former $P_{\rightarrow}$ domains. Upon cooling of the sample from temperatures above 510 K, no domain pattern is observed until bulk T_C is reached. This new domain sequence is independent from the primary one (not shown here).

Here, we report for the first time on the observation of a domain pattern of a clean BTO surface at temperatures above T_C. For BTO crystals prepared under ambient conditions, there are few studies also observing domain structures above T_C. The first PEEM experiments on BTO crystals by Le Bihan also revealed a high temperature pattern [13]. However, the surface could not be prepared free of contaminations [14]. Also in scanning surface potential microscopy, Kalinin and Bonnell could observe a domain structure at temperatures above T_C. This domain pattern decreases with time and has been explained by desorption of an adsorbate layer [15]. In contrast, our studies have been performed under UHV conditions to rule out the effect of adsorbates [16].

To gain insight into the origin in the experimentally observed work function contrast above T_C, we use first-principles density functional theory [17]. In detail, the Vienna *ab initio* simulation package (VASP) that solves the Kohn-Sham equations by using a plane wave basis set and projected augmented plane wave pseudopotentials has been applied [18]. In the calculations, the Brillouin zone is sampled by an $11 \times 11 \times 3$ k-point mesh. Furthermore, a cutoff energy of 500 eV is used. For structural relaxation, the Hellman-Feynman forces are calculated and minimized until 0.1 eV/Å. The primary concern of the calculations is to determine the differences in the work functions for the possible surface structures relevant for the experimentally observed photoemission contrast. In the following, we will compare the cubic paraelectric phase and the tetragonal ferroelectric phase with in-plane and out-of-plane polarizations in the vicinity of the BTO-vacuum interface.

For each domain type, slab calculations with 15 unit cells (u.c.) of BTO and 4 nm of vacuum have been performed. The top 5 u.c. are geometrically optimized, and the remaining layers are fixed. The different polarization directions are modeled by fixing the displacements of the unrelaxed layers to the corresponding direction and the bulk value of BTO [19]. For the surface, a TiO_2 termination is chosen here, since it is found to be energetically preferred [19–21].

Independent of the polarization direction, the topmost TiO_2 layer shows an outward relaxation of the oxygen. This finding originates from two effects. First, the missing Ti-O bonds at the surface with respect to bulk BTO cause an inward relaxation of Ti [19,20]. Second, the different ionic radii of oxygen and Ti have to equilibrate to allow for a flat isocharge surface [22]. In the case of $P_{\downarrow}$, there is nearly no surface relaxation, since the displacement is a continuation of the underlying bulk behavior. Similarly, for P_0 and $P_{\rightarrow}$, the surface layer rumbling causes only some minor distortions with respect to the bulk that vanish within the next 2 u.c. In the case of $P_{\uparrow}$, a strong relaxation is found that vanishes only after 3.5 u.c. This different behavior is due to the fact that the ferroelectric displacement is in contradiction with the surface relaxation.

Based on the approach of Neugebauer and Scheffler [23], the work functions corresponding to the different structures have been determined to 6.28, 4.92, and 5.95 eV for the ferroelectric $P_{\downarrow}$, $P_{\uparrow}$, and $P_{\rightarrow}$ states, respectively. The paraelectric P_0 results in 5.94 eV, very similar to the in-plane $P_{\rightarrow}$ state. The three different calculated work functions relate directly to the three PEEM intensities below T_C and show the same trend. However, the absolute averaged experimental work function of about 3.8 eV is significantly lower. This discrepancy is caused by the fact that the calculations assume surfaces of perfect composition, whereas a mild reduction of the $BaTiO_3$ crystal is necessary to get a sufficiently conducting sample enabling photoemission experiments. Details are discussed in Ref. [10].

For the assessment of the behavior above T_C, the experimental finding of a photoemission contrast inversion for former $P_{\downarrow}$ domains with respect to $P_{\rightarrow}$ domains points to a significant work function change. Two scenarios which would explain the experimental observation will be discussed. A surface-induced destabilization of the $P_{\downarrow}$ state which converts in a $P_{\uparrow}$-like state might explain the contrast inversion for $P_{\downarrow}$-$P_{\rightarrow}$ stripe domains and the constant contrast for $P_{\uparrow}$-$P_{\rightarrow}$ stripes. This explanation would suggest a ferroelectric surface layer above T_C with four stable in-plane and one stable out-of-plane polarization. An argument for this scenario is the observed continuation of the asymmetry at T_C between $P_{\uparrow}$ and $P_{\rightarrow}$ domains in Fig. 3(b). However, an alternative explanation is conceivable which is based on an energetically preferred ionic surface relaxation with a tetragonal distortion of the subsurface unit cells. As this influence becomes smaller with increasing distance from the surface, also the tetragonality decreases. The epitaxial misfit to the cubic symmetry of the bulk

unit cells causes stress within the surface layer. This stress is reduced by sequences of domains of alternating tetragonal distortions within and perpendicular to the surface plane. Thus, the former $P_{\downarrow}$ ($P_{\uparrow}$) stripes are constrained by the former $P_{\rightarrow}$ domains. Since also the domain structure at room temperature depends on the strain within the sample, the domain structure above T_C establishes domain walls at the same sample positions leading to a very similar domain pattern. Upon further temperature increase, also the subsurface unit cells continuously lose their tetragonality and finally become cubic. Density functional theory calculations for a paraelectric but out-of-plane tetragonally distorted BTO surface layer result in a work function of 5.73 eV, slightly below P_0 and $P_{\rightarrow}$, respectively. Based on this reasoning, former $P_{\downarrow}$ and $P_{\uparrow}$ domains appear equivalent above T_C and always show a higher photoemission intensity than former $P_{\rightarrow}$ domains. With increasing temperature, the tetragonal surface distortions decrease continuously with decreasing photoemission contrast. Finally, above 510 K, all unit cells adopt the same cubic structure and no work function contrast remains. In both scenarios, a surface-induced tetragonal distortion above T_C leads to the observed domain pattern. However, the existence of a switchable ferroelectric surface polarization is still unclear.

In conclusion, the high surface sensitivity of PEEM enables the characterization of ferroelectric domains at the surface of a well-prepared BTO (001) single crystal. A domain pattern well above the bulk phase transition temperature is observed, where $P_{\downarrow}$ domains are subject to a contrast inversion compared to $P_{\rightarrow}$ domains. The domain contrast which is based on local work function differences decreases continuously above T_C. The work function contrast is addressed by first-principles calculations for different BTO surface structures. The calculations indicate a tetragonal distortion of the surface-near unit cells which is stabilized by an ionic surface relaxation on top of a paraelectric cubic BTO bulk. The experimentally observed contrast above T_C can therefore be assigned to surface-near domains with in- and out-of-plane tetragonality without the necessity of a spontaneous polarization. These topmost unit cells transform continuously into the cubic state with increasing temperature.

This work was financially supported by the DFG through SFB 762. Technical support by Ralf Kulla and fruitful discussions with Mario Kiel are gratefully acknowledged.

*anke.hoefer@physik.uni-halle.de
†michael.fechner@mat.ethz.ch

[1] J. Mannhart and D. G. Schlom, Science **327**, 1607 (2010).
[2] E. Y. Tsymbal and H. Kohlstedt, Science **313**, 181 (2006).
[3] H. Zheng *et al.*, Science **303**, 661 (2004).
[4] R. Ramesh and N. A. Spaldin, Nature Mater. **6**, 21 (2007).
[5] M. Anliker, H. R. Brugger, and W. Känzig, Helv. Phys. Acta **27**, 99 (1954).
[6] W. J. Merz, J. Appl. Phys. **27**, 938 (1956).
[7] M. E. Drougard and R. Landauer, J. Appl. Phys. **30**, 1663 (1959).
[8] S. K. Streiffer, C. Basceri, C. B. Parker, S. E. Lash, and A. I. Kingon, J. Appl. Phys. **86**, 4565 (1999).
[9] A. F. Santander-Syro *et al.*, Nature (London) **469**, 189 (2011).
[10] A. Höfer, K. Duncker, M. Kiel, S. Förster, and W. Widdra, IBM J. Res. Dev. **55**, 4:1 (2011).
[11] L. Wegmann, Mikroskopie **26**, 99 (1970).
[12] S. V. Kalinin and D. A. Bonnell, Phys. Rev. B **63**, 125411 (2001).
[13] R. Le Bihan, C. R. Hebd. Seances Acad. Sci., Ser. B **275**, 29 (1972).
[14] M. Maussion and R. LeBihan, Ferroelectrics **26**, 847 (1980).
[15] S. V. Kalinin and D. A. Bonnell, J. Appl. Phys. **87**, 3950 (2000).
[16] To exclude significant dynamical effects, PEEM images have been recorded at an elevated temperature of approximately 420 K for 100 min. No time-dependent changes of the domain pattern have been observed.
[17] W. Zhong, D. Vanderbilt, and K. M. Rabe, Phys. Rev. Lett. **73**, 1861 (1994).
[18] G. Kresse and J. Furthmüller, Comput. Mater. Sci. **6**, 15 (1996).
[19] M. Fechner, S. Ostanin, and I. Mertig, Phys. Rev. B **77**, 094112 (2008).
[20] R. I. Eglitis and D. Vanderbilt, Phys. Rev. B **76**, 155439 (2007).
[21] Note that the conclusions here do not depend on the specific termination. The trend in the work function has been verified also for a BaO surface termination.
[22] H. L. Meyerheim, F. Klimenta, A. Ernst, K. Mohseni, S. Ostanin, M. Fechner, S. Parihar, I. V. Maznichenko, I. Mertig, and J. Kirschner, Phys. Rev. Lett. **106**, 087203 (2011).
[23] J. Neugebauer and M. Scheffler, Phys. Rev. B **46**, 16 067 (1992).